

A Kinetic Study of the Ring-Opening Process in Tungsten Carbonyl Complexes Containing Hemilabile Metallodithiolate Ligands

Andrea L. Phelps, Marilyn V. Rampersad, Shawn B. Fitch, Marcetta Y. Darensbourg, and Donald J. Darensbourg*

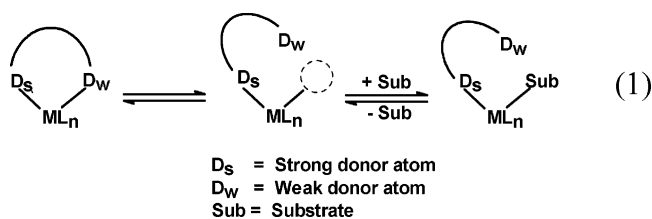
Department of Chemistry, Texas A&M University, College Station, Texas 77843

Received August 10, 2005

The synthesis of the metallodithiolate derivative of tungsten pentacarbonyl from the reaction of photogenerated $W(CO)_5THF$ and **Ni-1*** ((1,5-bis(2-mercapto-2-methylpropane)-1,5-diazacyclooctanato)nickel(II)) is described, along with its crystal structure. In *N,N*-dimethylformamide solution, the pentacarbonyl exists in equilibrium with its tetracarbonyl analogue and carbon monoxide. The pentacarbonyl complex stereoselectively loses cis carbonyl ligands, as is apparent from ^{13}CO -labeling studies, where the thus-formed tetracarbonyl tungsten complex resulting from chelate ring-closure is preferentially ^{13}CO -labeled among the two mutually trans CO groups. The kinetics of the addition of CO to the tetracarbonyl to afford the metal pentacarbonyl were monitored by means of in situ infrared spectroscopy in the ν_{CO} region at CO pressures between 28 and 97 bar and temperatures over the range 45–60 °C. Under these conditions, there was no evidence for W–S bond cleavage in the pentacarbonyl complex with concomitant formation of $W(CO)_6$. These studies reveal that the tetracarbonyl complex and CO are only slightly unstable with respect to the formation of the pentacarbonyl complex, with an equilibrium constant at 50 °C of about $2.8 M^{-1}$ or $\Delta G^\circ = -1.4$ kJ/mol. The activation parameters determined for the ring-opening process ($\Delta H^\ddagger = 89.1$ kJ/mol and $\Delta S^\ddagger = -37.2$ J/mol·K) suggest a solvent-assisted concerted ring-opening mechanism.

Introduction

Homogeneous catalysis typically advances with specially designed ligands, such that subtle changes in chelate bite angle, steric or electronic features, and ligand flexibility enhance catalyst performance. A current and attractive class of chelate ligands for several important industrial processes simultaneously incorporates inert (strong binders to a particular metal) and labile (weak binders) donor groups on the same ligand.¹ Such “hemilabile” ligands may temporarily hold coordination sites on reactive metal centers and easily produce an open site with the labile donor group while the substitutionally inert group remains anchored to the metal center.^{1–3} The capability of reforming the catalytic resting state or precursor is, in theory, a process that should lead to greater catalyst stability and recovery, as well as specific catalysis enhancing properties (eq 1).

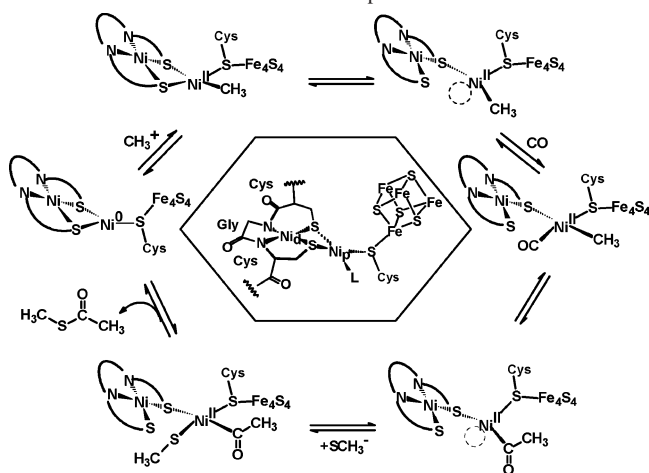


The variety of structural forms displayed in isolated and well-characterized polymetallic compounds derived from square planar NiN_2S_2 complexes as bidentate S-donor ligands suggests possible intermediates in their reaction chemistry.^{4–12}

* To whom correspondence should be addressed. Fax: (979) 845-0158. E-mail: djdarens@mail.chem.tamu.edu.

- (1) Slone, C. S.; Weinberger, D. A.; Mirkin, C. A. *Prog. Inorg. Chem.* **1999**, *48*, 233–350.
- (2) Jeffery, J. C.; Rauchfuss, T. B. *Inorg. Chem.* **1979**, *18*, 2658–2665.
- (3) Espinet, P.; Soulantica, K. *Coord. Chem. Rev.* **1999**, *193–195*, 499–556.

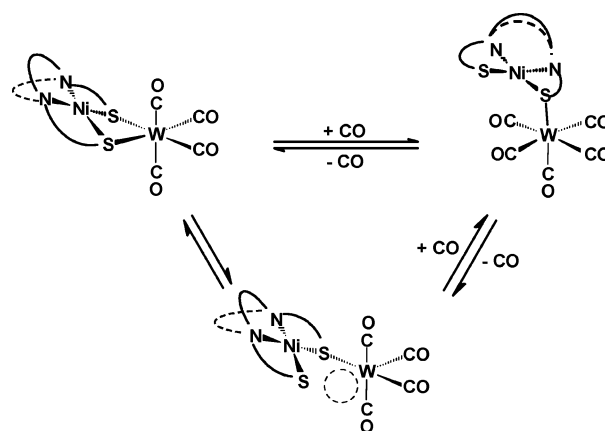
- (4) Jicha, D. C.; Busch, D. H. *Inorg. Chem.* **1962**, *1*, 872–877.
- (5) Lai, C.; Reibenspies, J. H.; Darensbourg, M. Y. *Angew. Chem., Int. Ed. Engl.* **1996**, *35*, 2390–2393.
- (6) Golden, M. L.; Jeffery, S. P.; Miller, M. L.; Reibenspies, J. H.; Darensbourg, M. Y. *Eur. J. Inorg. Chem.* **2004**, 231–236.
- (7) Rao, P. V.; Bhaduri, S.; Jiang, J.; Holm, R. H. *Inorg. Chem.* **2004**, *43*, 5833–5849.
- (8) Miller, M. L.; Ibrahim, S. A.; Golden, M. L.; Darensbourg, M. Y. *Inorg. Chem.* **2003**, *42*, 2999–3007.
- (9) Jeffery, S. P.; Lee, J.; Darensbourg, M. Y. *Chem. Commun.* **2005**, 1122–1124.
- (10) Hatlevik, Ø.; Blanksma, M. C.; Mathrubootham, V.; Arif, A. M.; Hegg, E. L. *JBIC* **2004**, *9*, 238–246.
- (11) Harrop, T. C.; Olmstead, M. M.; Mascharak, P. K. *Chem. Commun.* **2004**, 1744–1745.

Scheme 1. ACS Active Site and Computed Mechanism¹³

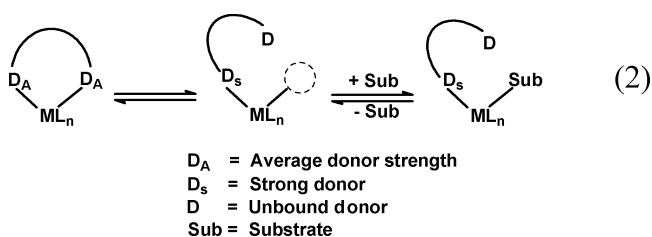
Our interest in this chemistry, as well as the possibility that the NiN_2S_2 complexes might serve as hemilabile ligands, was piqued by the recent computational mechanism designed to understand the role of a natural NiN_2S_2 metalloligand found within the binuclear active site of the acetyl-CoA synthase, ACS, enzyme; its structure is shown in Scheme 1.¹³ Computed stable species along the reaction path find that the chelating NiN_2S_2 ligand dissociates one sulfur donor, opening a site for CO addition, followed by methyl migration to form a metal-acetyl adduct. The CoA thiolate claims the available coordination site followed by reductive elimination of the thioester and completion of the catalytic cycle. Structural models of key intermediates and one functional model of a key step in this computed mechanism have been reported.^{14–16}

This report focuses on the observation that NiN_2S_2 complexes of $\text{W}(\text{CO})_4$ in which the nickel dithiolate serves as a bidentate S-donor ligand are readily converted in the presence of CO to a monodentate pentacarbonyl tungsten derivative, Scheme 2.¹⁷ This reversible process is of interest since the second $\text{W}-\text{S}$ bond dissociation and replacement by CO is a much slower or higher barrier process. Both processes, the NiS_2 -chelate ring-opening and the monodentate S-donor ligand loss, are expected, according to classical organometallic chemistry mechanisms, to proceed via a 16-electron, 5-coordinate intermediate in noncoordinating solvents. The lack of an anticipated contribution to the rate of these processes from an interchange pathway is because CO is a poor nucleophile and of low concentration at modest pressures in all organic and aqueous solvents. Thus, despite the original definition of hemilability which was coined for mixed-donor ligands, one donor being stronger than the other,

Scheme 2



we will maintain that the bidentate–monodentate conversion process exhibited by the NiN_2S_2 metallodithiolato ligands in the $(\text{NiN}_2\text{S}_2)\text{W}(\text{CO})_4$ complexes provides an example of hemilability, eq 2.



In recent studies of a series of $(\text{NiN}_2\text{S}_2)\text{W}(\text{CO})_4$ complexes designed to establish steric and electronic parameters for definition of NiN_2S_2 ligands, it was noted that the charge and substituents on the ligand control the extent of ring-opening in the presence of CO.¹⁷ As this fundamental aspect of the chemistry of such compounds would affect potential applications in catalysis,¹⁶ we have endeavored to place the hemilability of $(\text{NiN}_2\text{S}_2)\text{W}(\text{CO})_4$ on a semiquantitative basis through kinetic studies.

Experimental Section

Method and Materials. All manipulations were performed on a double-manifold Schlenk vacuum line under an atmosphere of nitrogen or in an argon-filled glovebox. Solvents were reagent grade and were dried and deoxygenated according to published procedures under a N_2 atmosphere.¹⁸ The **Ni-1***, *cis*- $\text{W}(\text{CO})_4(\text{pip})_2$ (pip = piperidine), and **[Ni-1*]** $\text{W}(\text{CO})_4$ complexes were synthesized according to published procedures.^{16,19,20} All other chemicals were purchased from Aldrich Chemical Co. and used as received. DMF was purchased from Acros Chemical Company.

Physical Measurements. Elemental analyses were performed by the Canadian Microanalytical Services, Ltd., Delta, British Columbia, Canada. Infrared spectra were recorded on a Bruker Tensor 27 FTIR spectrometer using a CaF_2 cell of 0.1-mm path length. Photolysis experiments were performed using a mercury arc 450W UV immersion lamp. High-pressure reaction kinetic measurements were carried out using a stainless steel Parr autoclave

(12) Reynolds, M. A.; Rauchfuss, T. B.; Wilson, S. R. *Organometallics* **2003**, *22*, 1619–1625.

(13) Webster, C. E.; Darensbourg, M. Y.; Lindahl, P. A.; Hall, M. B. *J. Am. Chem. Soc.* **2004**, *126*, 3410–3411.

(14) Linck, R. C.; Spahn, C. W.; Rauchfuss, T. B.; Wilson, S. R. *J. Am. Chem. Soc.* **2003**, *125*, 8700–8701.

(15) Krishnan, R.; Riordan, C. G. *J. Am. Chem. Soc.* **2004**, *126*, 4484–4485.

(16) Rampersad, M. V.; Jeffery, S. P.; Reibenspies, J. H.; Ortiz, C. G.; Darensbourg, D. J.; Darensbourg, M. Y. *Angew. Chem., Int. Ed.* **2005**, *44*, 1217–1220.

(17) Rampersad, M. V.; Jeffery, S. P.; Golden, M. L.; Lee, J.; Reibenspies, J. H.; Darensbourg, D. J.; Darensbourg, M. Y. *J. Am. Chem. Soc.* **2005**, *127*, ASAP.

(18) Gordon, A. J.; Ford, R. A. *The Chemist's Companion*; Wiley and Sons: New York, 1972; pp 429–436.

(19) Darensbourg, M. Y.; Font, I.; Pala, M.; Reibenspies, J. H. *J. Coord. Chem.* **1994**, *32*, 39–49.

(20) Darensbourg, D. J.; Kump, R. L. *Inorg. Chem.* **1978**, *17*, 2680–2682.

modified with a SiComp window to allow for attenuated total reflectance spectroscopy using infrared radiation (ASI ReactIR 1000 in situ probe).

Synthesis of [1,5-Bis(2-mercapto-2-methylpropane)-1,5-Diazacyclooctanato]nickel(II) Tungsten Pentacarbonyl, [Ni-1*]W(CO)₅. The W(CO)₆ (0.53 g, 1.49 mmol) and Ni-1* (0.52 g, 1.49 mmol) compounds were added to a degassed photolysis vessel under an N₂ atmosphere. To the solids were added 90 mL of THF and 40 mL of CH₂Cl₂, precooled to 10 °C. The solution was photolyzed for 30 min to yield a mixture of [Ni-1*]W(CO)₅ with a small amount of [Ni-1*]W(CO)₄. The reaction mixture was concentrated to about 10 mL, and the product was purified by alumina column chromatography with CH₂Cl₂ as the eluent. The solvent was removed by rotary evaporation to yield a brown solid (0.64 g, 64%). X-ray-quality crystals were obtained by vapor diffusion of ether into a CH₂Cl₂ solution of the product. Anal. Calcd (Found) for C₁₉H₂₈N₂Ni₁O₅S₂W₁: C, 34.00 (33.94); H, 4.21 (4.27); N, 4.17 (4.18). ¹³C NMR (DMF): 200.1 (equatorial), 202.1 (axial) ppm. IR (CH₂Cl₂, cm⁻¹) ν(CO): 2064 (w), 1976 (w), 1920(s), 1882 (m), DMF: 2061(w), 1971 (w), 1920 (s), 1874(m) cm⁻¹.

In Situ ReactIR Monitoring of CO Addition. In a typical experiment, 10 mL of DMF previously dried over molecular sieves was delivered via the injection port into a 300-mL stainless steel Parr autoclave reactor which had been dried overnight in vacuo maintained at 80 °C. The reactor is modified with a 30 bounce SiCOMP window to allow for the use of an ASI ReactIR 1000 system equipped with a MCT detector. The reactor was cooled to the appropriate temperature before the background solvent was injected. After time was allowed for the solvent to reach temperature, a single 128-scan background spectrum was collected. The complex, dissolved in 5 mL DMF, was injected into the reactor; and a single scan was collected. The reactor was then pressurized to the appropriate CO pressure, and one spectrum was collected every 3 min over a 10-h period. Profiles of the absorbance at 1920 cm⁻¹ with time were recorded after baseline correction and analyzed to provide rate constants. (Note: CO pressure and temperature varied within each experiment and are described in Results and Discussion.)

X-Ray Structure Analysis. The X-ray data were obtained from the Crystal and Molecular Structure Laboratory Center for Chemical Characterization and Analysis at Texas A&M University. The crystals were mounted on a glass fiber at room temperature. X-ray data were obtained on a Bruker P4 diffractometer. The space groups were determined on the basis of systematic absences and intensity statistics.²¹ The structures were solved by direct methods. Anisotropic displacement parameters were determined for all non-hydrogen atoms. Programs used for data collection and cell refinement, Bruker XSCANS; for data reduction, SHELXTL; for structure solution, SHELXS-97²² (Sheldrick); for structure refinement, SHELXL-97²³ (Sheldrick); and for molecular graphics and preparation of material for publication, SHELXTL-Plus, version 5.1 or later (Bruker).²⁴

(21) Sheldrick, G. *SHELXTL-PLUS revision 4.11V, SHELXTL-PLUS users manual*; Siemens Analytical X-ray Inst., Inc.: Madison WI, 1990.

(22) Sheldrick, G. *SHELXS-97 Program for Crystal Structure Solution*; Institut für Anorganische Chemie der Universität: Göttingen, Germany, 1997.

(23) Sheldrick, G. *SHELXL-97 Program for Crystal Structure Refinement*; Institut für Anorganische Chemie der Universität: Göttingen, Germany, 1997.

(24) *SHELXTL, version 5.1 or later*; Bruker Analytical X-ray Systems: Madison, WI, 1998.

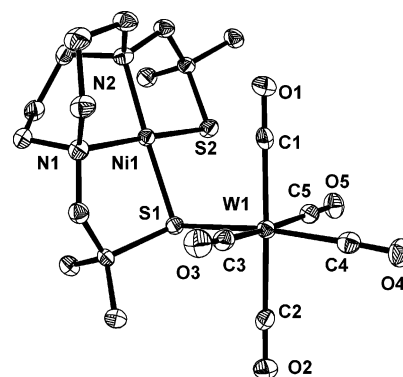


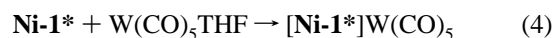
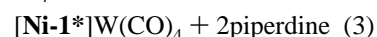
Figure 1. Thermal ellipsoid plots (50% probability) of [Ni-1*]W(CO)₅ with select atoms labeled and hydrogen atoms omitted.

Table 1. Selected Bond Distances and Bond Angles of the [Ni-1*]W(CO)₅ Complex with [Ni-1*]W(CO)₄ and Ni-1* Data Included for Comparison

	[Ni-1*]W(CO) ₅	[Ni-1*]W(CO) ₄	Ni-1*
Bond Distances, Å			
W(1)–C(1)	2.034(5)	2.001(14)	
W(1)–C(2)	2.060(5)	2.037(12)	
W(1)–C(3)	2.030(6)	1.951(10)	
W(1)–C(4)	1.980(5)	1.951(10)	
W(1)–C(5)	2.068(5)		
W(1)–S(1)	2.576(14)	2.589(3)	
Ni–S(1)	2.173(15)	2.170(3)	2.152(1)
Ni–S(2)	2.156(15)	2.170(3)	2.152(1)
Ni–N(1)	2.014(4)	1.986(3)	1.995(3)
Ni–N(2)	1.993(4)	1.986(3)	1.995(3)
Bond Angles, deg			
Ni(1)–S(1)–W(1)	107.95(5)	90.39(11)	
S(1)–Ni–S(2)	88.36(6)	87.62(15)	88.8(1)
N(1)–Ni–N(2)	90.67(18)	92.2(5)	90.4(1)
N(1)–Ni–S(1)	90.68(13)		
N(2)–Ni–S(2)	90.42(13)		
W(1)–C(1)–O(1)	176.5(4)	171.5(13)	
W(1)–C(2)–O(2)	176.2(5)	173.3(12)	
W(1)–C(3)–O(3)	177.2(4)	178.7(8)	
W(1)–C(4)–O(4)	177.7(4)	178.7(8)	
W(1)–C(5)–O(5)	178.5(5)		

Results and Discussion

We have recently reported a detailed account of the synthesis of various [NiN₂S₂]W(CO)₄ derivatives prepared by the labile ligand-displacement route indicated in eq 3 specifically for NiN₂S₂ = Ni-1* or 1,5-bis(2-mercapto-2-methylpropane)-1,5-diazacyclooctanonickel(II).¹⁶ Similarly, the [Ni-1*]W(CO)₅ derivative was prepared in situ from the photochemically generated W(CO)₅THF species (eq 4). The X-ray crystallographically derived structure of complex **1** has been published;¹⁶ the solid-state structure of complex **2** is described herein. Crystal data and details of collection parameters are provided in the Supporting Information. A thermal ellipsoid representation of complex **2** is found in Figure 1, with selected bond distances and angles reported in Table 1. Included in Table 1 for comparison are selected metric data for the free metallathiolate ligand Ni-1* and the [Ni-1*]W(CO)₄ complex.



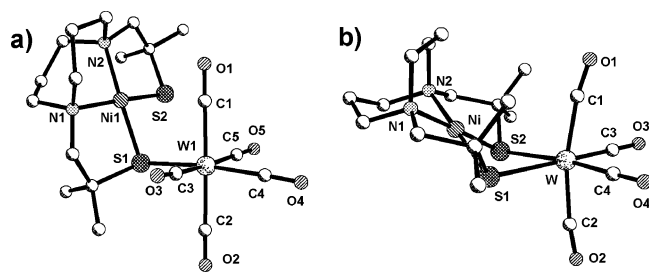
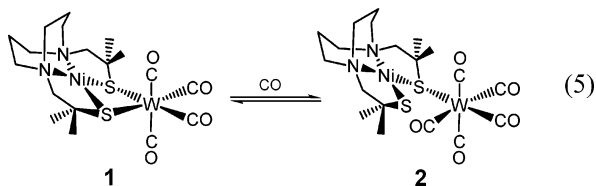


Figure 2. Structural comparison of ball-and-stick representation for the molecular structures (a) $[\text{Ni-1}^*]\text{W}(\text{CO})_5$ and (b) $[\text{Ni-1}^*]\text{W}(\text{CO})_4$.

The solid-state molecular structure of $[\text{Ni-1}^*]\text{W}(\text{CO})_5$ shows the tungsten pentacarbonyl derivative to exist as a distorted octahedron with the Ni-1^* moiety coordinated to tungsten in a monodentate fashion via one of its thiolate donors. The nickel atom remains in its square planar N_2S_2 coordination environment, similarly to that of the NiN_2S_2 free ligands and its tungsten tetracarbonyl derivatives.¹⁶ There are only minimal differences in the metric parameters in the tetracarbonyl and pentacarbonyl complexes. However, the ring-opened metallodithiolate ligand of the latter derivative results in a $\text{Ni}(1)-\text{S}(1)-\text{W}(1)$ angle of 108° , which is about 18° greater than that observed in the tetracarbonyl complex ($\text{Ni}(1)-\text{S}(1)-\text{W}(1) = 90^\circ$), thereby extending the $\text{Ni}\cdots\text{W}$ separation by ~ 0.5 Å from that observed in the $[\text{Ni-1}^*]\text{W}(\text{CO})_4$ complex ($\text{Ni}\cdots\text{W} = 3.389$ Å). This is best seen in the ball-and-stick drawings of the two complexes depicted in Figure 2. The four $\text{W}-\text{C}$ bonds cis to the S -donor have an average bond length of $2.048(5)$ Å with a range of 2.030 – 2.068 Å; the trans $\text{W}-\text{C}$ distance is, as expected, shorter at $1.980(5)$ Å. Both the $\text{Ni}-\text{N}(1)$ ($2.014(4)$ Å) and $\text{Ni}-\text{S}(1)$ ($2.173(15)$ Å) bond distances increase upon thiolate coordination to tungsten, while the $\text{Ni}-\text{N}(2)$ and $\text{N}-\text{S}(2)$ bonds remain the same as those in the free metallodithiolate ligand. The $\text{W}-\text{S}$ bond length of $2.576(14)$ Å is slightly, but not significantly, shorter than that seen for the $\text{W}-\text{S}$ bonds in $[\text{Ni-1}^*]\text{W}(\text{CO})_4$ of $2.589(3)$ Å.

The $\text{NiN}_2\text{S}_2\text{W}(\text{CO})_4$ complexes have been shown to undergo reaction with carbon monoxide to provide the corresponding $\text{NiN}_2\text{S}_2\text{W}(\text{CO})_5$ complex, in which only one arm of the chelating metallodithiolate is bound to the tungsten center.¹⁷ This process is depicted in eq 5 specifically for the



$[\text{Ni-1}^*]\text{W}(\text{CO})_4$ derivative and represents the focus of the kinetic study reported herein. Because of the limited solubility of carbon monoxide in organic solvents, we have carried out these investigations at moderate pressures of CO (400–1400 psi or 28–97 bar) employing a 300-mL stainless steel Parr reactor modified to accommodate an ASI ReactIR SiComp probe in DMF solvent. The infrared spectra of complexes **1** and **2** in the $\nu(\text{CO})$ region exhibit intense bands at 1996 , 1871 , 1857 , and 1816 cm^{-1} ; and 2061 , 1920 , and

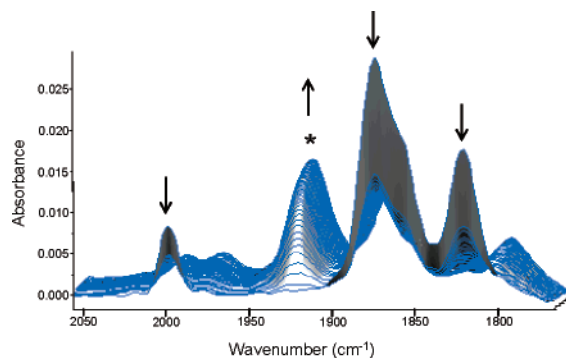


Figure 3. Three-dimensional stack plot of the IR spectra collected during the reaction of complex **1** and CO. The peak marked with an asterisk corresponds to the ν_{CO} band at 1920 cm^{-1} in the product, complex **2**.

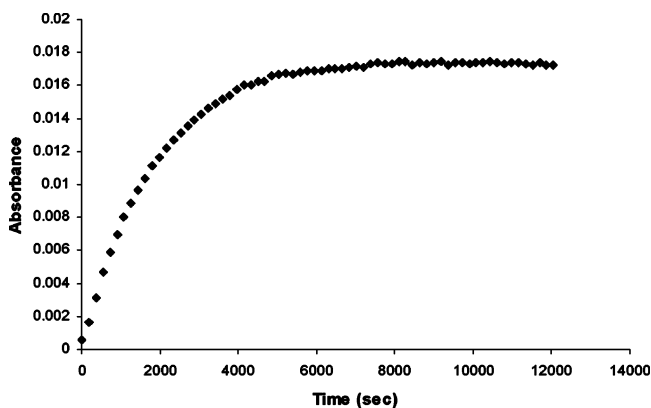


Figure 4. Reaction profile for the formation of complex **2** at 1400 psi of CO at 50° in DMF. Absorbance data measured at 1920 cm^{-1} .

1874 cm^{-1} in DMF, respectively. Figure 3 displays the three-dimensional stack plot of the infrared spectra collected every 3 min for a typical reaction of complex **1** with CO. The substitution reaction was monitored by following the appearance of the strong, isolated ν_{CO} vibrational mode at 1920 cm^{-1} in the product, complex **2**.

It is apparent from these studies that the reaction in eq 5 does not go to completion under the conditions employed. Even at 1400 psi of carbon monoxide at 50°C , there is an equilibrium distribution of complex **1** + CO and complex **2**. Furthermore, the once-formed pentacarbonyl tungsten derivative does not readily undergo reaction with CO to afford $\text{W}(\text{CO})_6$ at temperatures less than 60°C . This latter observation is indicative of the stability or inertness of the $\text{W}-\text{S}$ bond in the $\text{NiN}_2\text{S}_2\text{W}(\text{CO})_5$ complex. Figure 4 illustrates the reaction profile obtained upon monitoring the 1920 cm^{-1} ν_{CO} band in complex **2** with time by way of in situ infrared spectroscopy for a representative reaction, in this case at 1400 psi and 50°C . The $(\mu\text{-SR})/\text{CO}$ ligand-substitution reaction was demonstrated to be first-order in complex **1** via curve fitting of the data as described in Figure 5. That is, these data revealed a first-order dependence on complex **1** and provide a k_{obsd} from the equation $\ln(A_\infty - A_t) = -k_{\text{obsd}}t + \ln(A_\infty - A_0)$. A_∞ and A_t are the absorbance of the product, complex **2**, at $t = \infty$ and $t = \text{time}$.

The k_{obsd} values as a function of pressure of CO are compiled in Table 2. As is obvious from the plot of these data in Figure 6, the substitution reaction in eq 5 exhibits saturation kinetics as the $[\text{CO}]$ approaches infinity. This

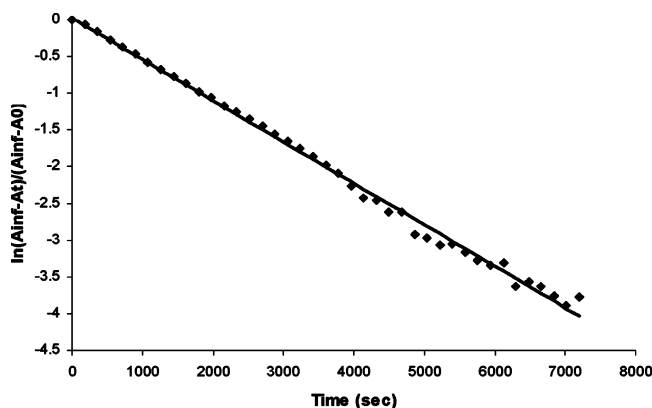


Figure 5. First-order plot of the conversion of complex **1** + CO to complex **2**. Reaction carried out in DMF at 50 °C under 1400 psi of CO.

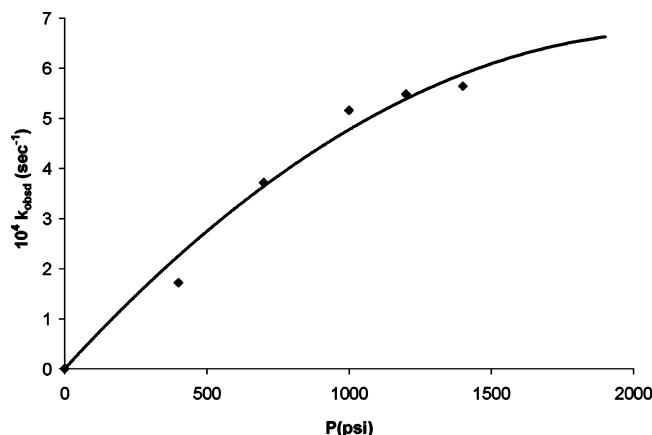


Figure 6. Plot of k_{obsd} vs CO pressure for reactions carried out at 50 °C.

Table 2. The Pseudo-First-Order Rate Constants, k_{obsd} , for the Reaction of Complex **1** with CO at 50 °C as a Function of CO Pressure^a

$10^4 k_{\text{obsd}}, \text{s}^{-1}$	$P_{\text{CO}}, \text{psi (bar)}$
1.72	400 (27.6)
3.72	700 (48.3)
5.16	1000 (69.0)
5.48	1200 (82.8)
5.64	1400 (96.6)

^a Estimated errors in k_{obsd} values are $\pm 7\%$.

observation is consistent with a dissociative process as outlined in Scheme 3, where chelate ring-closure competes with CO capture of the five-coordinate intermediate afforded upon W–S bond cleavage.

The predicted pseudo-first-order rate constant (k_{obsd}) for this mechanism is shown in eq 6, assuming **I** is a very reactive intermediate which, via the steady-state approximation, will disappear as rapidly as it is formed. When $k_2[\text{CO}] \gg k_{-1}$, $d[\mathbf{1}]/dt = -k_1[\mathbf{1}]$ or at “saturation kinetic” at 50 °C from Figure 6, $k_1 \approx 6.0 \times 10^{-4} \text{ s}^{-1}$.

$$-\frac{d[\mathbf{1}]}{dt} = \frac{d[\mathbf{2}]}{dt} = \left\{ \frac{k_1 k_2 [\text{CO}] + k_{-1} k_{-2}}{k_{-1} + k_2 [\text{CO}]} \right\} [\mathbf{1}] = k_{\text{obsd}} [\mathbf{1}] \quad (6)$$

The carbon monoxide concentration in *N,N*-dimethylformamide has been reported at 10.6 and 19.6 bar for temperatures between 393 and 433 K.²⁵ The [CO] determined at 393 K, the closest temperature to those employed in this study, was determined to be 4.85×10^{-2} and 9.68×10^{-2}

Scheme 3

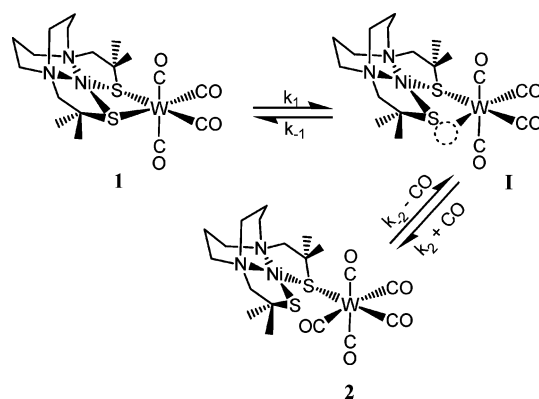


Table 3. The Pseudo-First-Order Rate Constant, k_{obsd} , for the Reaction of Complex **1** with CO at 55 bar Pressure as a Function of Temperature^a

$10^4 k_{\text{obsd}}, \text{s}^{-1}$	temp (K)
1.75	318
2.85	323
4.88	328
8.33	333

^a Estimated errors in k_{obsd} are $\pm 7\%$.

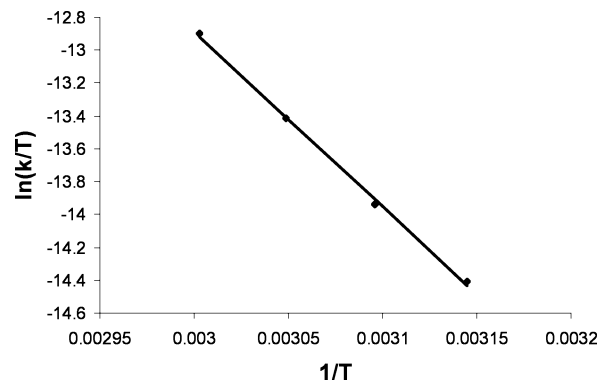
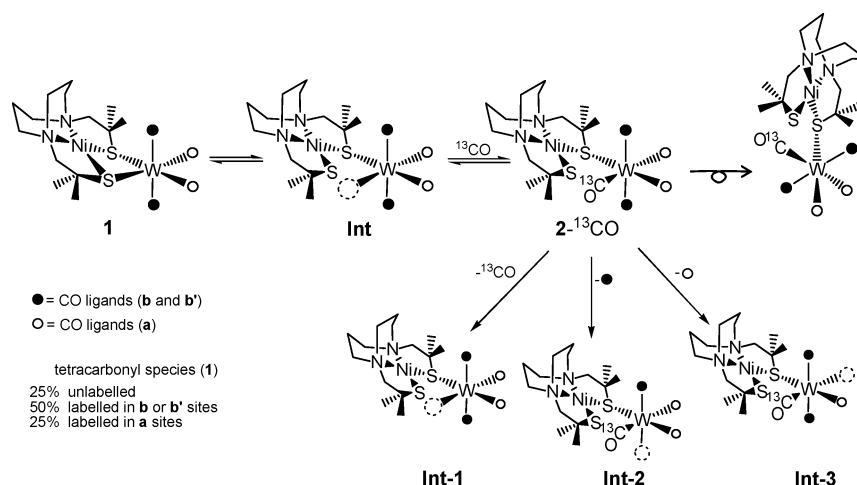


Figure 7. Eyring plot for the conversion of complex **1** + CO \rightarrow **2**.

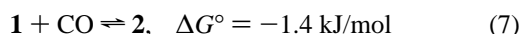
M at 10.6 and 19.6 bar, respectively. Since [CO] varies linearly with pressure and increases with an increase in temperature, we can estimate the maximum [CO] in DMF at 50 °C (323 K) to be 0.13 M at 27.6 bar and 0.47 M at 96.6 bar. For entries 1 and 5 in Table 2, we have determined the ratio of $[\mathbf{2}]/[\mathbf{1}]$ at equilibrium to be 0.408 and 1.13, respectively. Hence, the equilibrium constant for the reaction defined in eq 5 is expected to be slightly greater than 3.1 or 2.4 at 50 °C. In other words the $K_{\text{eq}}(\text{ave}) = 2.8 \text{ M}^{-1}$ or the reaction with a ΔG° of about -1.4 kJ/mol at 50 °C is almost thermodynamically neutral (eq 7). The composite activation parameters determined from the data in Table 3 for the process in eq 5 from a reaction carried out at 800 psi (55 bar) of carbon monoxide (see Eyring plot in Figure 7) were $\Delta H^\ddagger = 89.1 \text{ kJ/mol}$ and $\Delta S^\ddagger = -37.2 \text{ J/mol}\cdot\text{K}$. These activation parameters represent those associated with the metathiolate ring-opening process, with concomitant reaction of the tungsten center with CO and formation of $[\text{Ni-1}^*]\text{W}(\text{CO})_5$. The quite negative entropy of activation determined for this reaction, which was carried out in the polar,

(25) Khan, M. M. T.; Halligudl, S. B.; Shukla, S. J. *Chem. Eng. Data* **1989**, *34*, 353–355.

Scheme 4



aprotic solvent DMF, is most likely due to a solvent-assisted concerted ring-opening mechanism. Dobson and co-workers have demonstrated such a mechanism for ring-opening four-membered chelated dithioether derivatives of Mo and W in the presence of alkyl and aryl phosphites.^{26–28}



Upon carrying out the reaction outlined in Scheme 3 in the presence of ^{13}C O (slightly greater than 1 bar), an interesting observation was made. The rate of ^{13}C O incorporation into complex **1**, as the result of the thus-formed ^{13}C O-labeled complex **2** undergoing CO loss, is stereoselective. This is evidenced by the ^{13}C NMR spectra, which clearly show that the two mutually trans CO groups are isotopically enriched at a faster rate than the two CO groups trans to sulfur donors (see Figure 8). The nonequivalence of the two axial CO

groups has been shown to be the result of the unique orientation of the NiN_2S_2 ligand with respect to the $\text{W}(\text{CO})_4$ unit.¹⁷ Scheme 4 summarizes this observation, where the initially produced $2\text{-}^{13}\text{C}$ O, the pentacarbonyl derivative labeled in the position cis to the S-donor, undergoes stereoselective loss of one of the equatorial CO ligands. The three possibilities for the rigid 5-coordinate intermediate are shown as **Int-1**, **Int-2**, and **Int-3**, produced in the ratio 1:2:1. Ring-closure in the initial stages of the reaction would thus result in twice as much ^{13}C O enrichment in the **b** or **b'** positions as in the **a** position. That is, ring-closure of **Int-2** and **Int-3** would lead to a ^{13}C O label in **b** or **b'** and **a**, respectively.

The stereoselective loss of carbonyl groups cis to the sulfur donor ligand in complex **2** is consistent with the cis-labilization arguments of Brown and co-workers.²⁹ In addition, the distal sulfur donor may assist the dissociation of a cis carbonyl ligand, as has been proposed for other mono-coordinated, potentially chelating ligands, such as carboxylates.³⁰ Indeed, the distal sulfur donor in the solid-state structure of **2** is within the sum of the van der Waals radii of the sulfur and carbon atoms ($\text{S}(2)\cdots\text{C}(5) = 3.49 \text{ \AA}$, whereas the sum of van der Waals radii = 3.50 \AA). More importantly, this nonbonding distance is minimized to an average $\text{S}\cdots\text{C}$ separation of 3.20 \AA upon allowing free rotation about the $\text{W}-\text{S}$ bond, as would be expected in solution (see space-filling model in Figure 9).³¹ Other reports of possible interactions between distal donors (N, P) with cis carbonyl ligands have been published.³²

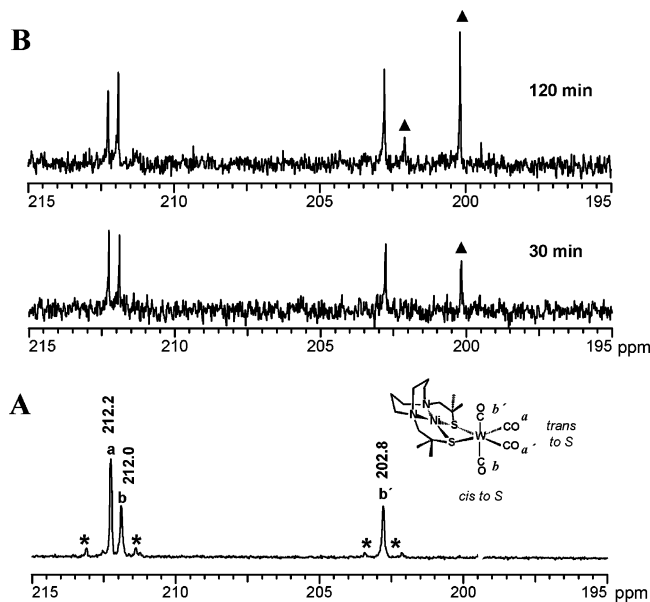


Figure 8. (A) Natural-abundance ^{13}C NMR spectrum of CO resonances in complex **1**. Note: Ratio of combined equatorial CO signals (**b** and **b'**) to the axial CO signal (**a**) is 1.0. Peaks marked by asterisks correspond to $^{183}\text{W}-^{13}\text{C}$ coupling. (B) ^{13}C NMR spectra of carbonyl resonances resulting from $1 + ^{13}\text{C}\text{O} \rightleftharpoons 2$. After 30 and 120 min reaction periods at 50°C in DMF the ratios of (**b** and **b'**)/**a** are 1.80 and 2.70, respectively. Peaks marked with \blacktriangle at 202.1 and 200.1 ppm are due to ^{13}C O-enriched complex **2**.

- (26) Dobson, G. R.; Faber, G. C. *Inorg. Chem.* **1968**, *7*, 584–588.
- (27) Awad, H. H.; Dobson, C. B.; Dobson, G. R.; Leipoldt, J. G.; Schneider, K.; van Eldik, R.; Wood, H. E. *Inorg. Chem.* **1989**, *28*, 1654–1657.
- (28) Dobson, G. R.; Cortés, J. E. *Inorg. Chem.* **1988**, *27*, 3308–3314.
- (29) (a) Atwood, J. D.; Brown, T. L. *J. Am. Chem. Soc.* **1976**, *98*, 3160–3166. (b) Atwood, J. D.; Brown, T. L. *J. Am. Chem. Soc.* **1975**, *97*, 3380–3385. (c) Atwood, J. D.; Brown, T. L. *J. Am. Chem. Soc.* **1976**, *98*, 3155–3159. (d) Cohen, M. A.; Brown, T. L. *Inorg. Chem.* **1976**, *15*, 1417–1423. (e) Lichtenberger, D. L.; Brown, T. L. *J. Am. Chem. Soc.* **1978**, *100*, 366–373.
- (30) (a) Darensbourg, D. J.; Wiegrefe, H. P.; Wiegrefe, P. W. *J. Am. Chem. Soc.* **1990**, *112*, 9252–9257. (b) Darensbourg, D. J.; Joyce, J. A.; Bischoff, C. J.; Reibenspies, J. H. *Inorg. Chem.* **1991**, *30*, 1137–1142.
- (31) We are indebted to Dr. J. H. Reibenspies for the molecular mechanic computation using PC Model for Windows, Version 6.0, Serena Software.

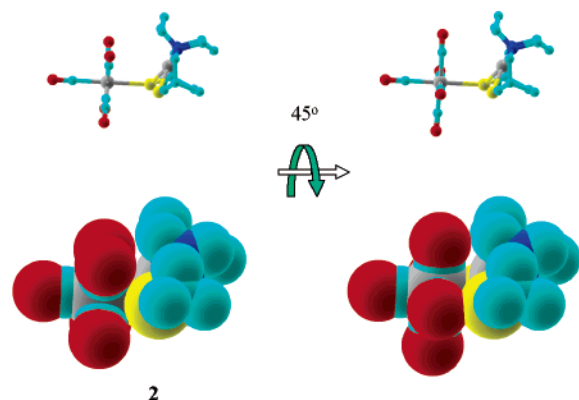
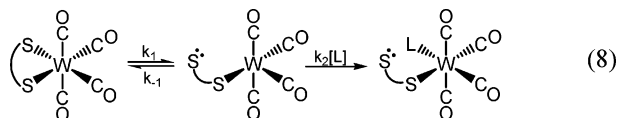


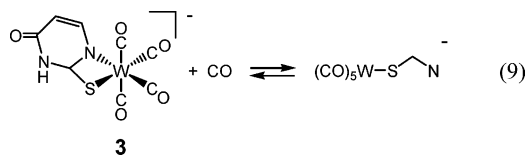
Figure 9. Space-filling model of complex **2** and **2** with the thiolate ligand rotated to show van der Waals contact of distal sulfur atom with the carbon atom of one of the equatorial CO ligands.

It has long been recognized that the high kinetic stability of chelation decreases as the chelate ring size increases.³³ This phenomenon is thought to arise from the fact that the rate constant for chelate ring-opening increases as the chelate ring size increases. Relevant to our study, the rate constant (k_1) for chelate ring-opening of the six-membered chelate ring in ($\text{BuS}(\text{CH}_2)_m\text{S}'\text{Bu}$) $\text{W}(\text{CO})_4$ ($n = 3$) was shown to be 40-fold times faster than its five-membered analogue ($n = 2$).³⁴ These kinetic data were determined for the process skeletally outlined in eq 8, where the incoming ligand was tris(isopropyl)phosphite. The increase in the rate of ring-opening was rationalized on the basis of structural data for the two derivatives which indicated that there was greater ring distortions in the six-membered complex, as evidenced by a smaller S–W–S angle, shorter nonbonded S...S distance, and a longer average W–S bond length.³⁵ On the other hand, the rate constants for ring-closure (k_{-1}) in the two derivatives were similar at $2.04(3) \times 10^5$ and $5.67(2) \times 10^5 \text{ s}^{-1}$, respectively.



There is little comparative kinetic data for related ring-opening reactions involving a four-membered, metallochelate ring system as employed in our study. However, the ring distortions (deviations from the 90° angles of octahedral geometry) in complex **2** are greater than those found in the ($\text{BuS}(\text{CH}_2)_3\text{S}'\text{Bu}$) $\text{W}(\text{CO})_4$ derivative (values listed in brackets), e.g., in **2**, the S–W–S = $70.92(12^\circ)$ [$79.1(1)^\circ$], the nonbonding S...S distance = 3.017 \AA [$3.284(7) \text{ \AA}$], and W–S = $2.589(3) \text{ \AA}$ [$2.578(5) \text{ \AA}$]. Nevertheless, the rate constants for ring-opening in these two systems are quite

similar at 35.2°C ($k_1 = 6.5$ vs $5.7 \times 10^{-5} \text{ s}^{-1}$). A significant difference in the two systems might have been expected because of the enhanced release of strain upon ring-opening in **2**. However, there is little flexibility of the S...S chelate in complex **2** because of the rigorously planar $\text{N}_2\text{S}_2\text{Ni}$ complex, and hence a greater gain in the degrees of freedom should be experienced upon ring-opening of the dithioether ligand. The stability of the W–S bond in complex **2**, i.e., its resistance to bond cleavage, is further evidenced from a comparison of the rate constant for ring-opening the four-membered chelate in the $\text{W}(\text{CO})_4(2\text{-thiouracilate})^-$ anion (**3**), eq 9.³⁶ In this instance, the ring-opening rate constant for W–N bond dissociation in the presence of CH_3CN was determined to be $\sim 1.2 \times 10^{-3}$ at 35°C , or 2 orders of magnitude faster than that observed in the $[\text{Ni-1}^*]\text{W}(\text{CO})_4$ process. Similar to the lack of further reactivity of the W–S bond toward displacement in complex **2**, the pentacarbonyl complex afforded from reaction 9 was stable with regard to W–S bond cleavage.



Concluding Remarks

Kinetic parameters determined for the formation of $[\text{Ni-1}^*]\text{W}(\text{CO})_5$ from the addition of CO to its tetracarbonyl analogue clearly demonstrate that, although ring-opening is a rather facile process, the once-formed pentacarbonyl derivative is extremely stable toward further W–S bond cleavage. This property of a chelated ligand is of course a highly desirable feature for catalytic processes which involve chelate ring-opening to provide a site for substrate binding and further reaction. Indeed, in metal complexes of higher oxidation states, e.g., Pd(II) or Pt(II) where the metal–S bond is stronger, the stability of the ring-opened form with substrate added might be anticipated to be even greater than that observed for the W(0) derivative. A factor opposing the catalytic efficiency of these metallodithiolate ligand systems is the observation that the chelated derivative in the presence of a good substrate (modeled by CO in our studies) is essentially thermodynamically neutral with regard to formation of the substrate-bound metal complex. Nevertheless, by employing high concentrations of substrate, this phenomenon might be kinetically overcome. Of importance to catalytic processes, these metallodithiolate ligands, because of their spatial and orientational requirements, are likely to impart regioselective substrate binding and reaction.

Of relevance to the active site of the ACS enzyme, preliminary studies of the $\text{W}(\text{CO})_4$ derivative of the $\text{Ni}(\text{ema})^{2-}$ ligand ($\text{ema}^{4-} = N,N'$ -ethylenebis(2-mercaptoacetamide)) finds ring-opening in the presence of CO to occur at a much faster rate than that noted above for the neutral Ni-1^* ligand. This observation is quite reasonable since dissociation of the

(32) (a) Bibal, C.; Smurny, Y. D.; Pink, M.; Caulton, K. G. *J. Am. Chem. Soc.* **2005**, *127*, 8944–8945. (b) Benson, J. W.; Keiter, R. L.; Keiter, E. A.; Rheingold, A. L.; Yap, G. P. A.; Mainz, V. V. *Organometallics* **1998**, *17*, 4275–4281.
 (33) Martell, A. E.; Smith, R. M. *Critical Stability Constants*; Plenum: New York, 1977; Vol. 2.
 (34) Dobson, G. R.; Basson, S. S.; Dobson, C. B. *Inorg. Chim. Acta* **1985**, *105*, L17–L19.
 (35) Reisner, G. M.; Bernal, I.; Dobson, G. R. *J. Organomet. Chem.* **1978**, *157*, 23–39.

(36) Darensbourg, D. J.; Frost, B. J.; Derecskei-Kovacs, A.; Reibenspies, J. H. *Inorg. Chem.* **1999**, *38*, 4715–4723.

dianionic ligand would relieve the excess electron density donated to the W(0) center by the dianionic ligand, thereby opening a site for the good π acceptor CO to bind. Again, in this instance, complete ligand dissociation did not occur, further affirming that the remaining W–S bond is strengthened upon chelate ring-opening. The hemilability of the biomimetic ligand Ni(ema)²⁻ suggests that the Ni(CysGlyCys)²⁻ ligand found in nature might also possess this property, thus supporting the theoretical mechanism put forth by Webster and co-workers.¹³ It should be noted that in the natural system the N-to-S linkers are asymmetric, which could lead to preferential ring-opening of one of the Ni–S bonds.

Acknowledgment. We gratefully acknowledge the financial support from the National Science Foundation (CHE 01-11629 and CHE 02-34860), Robert A. Welch Foundation, and National Institute of Health for the Ruth L. Kirschstein–NRSA Fellowship (F31 GM073350-01).

Supporting Information Available: X-ray crystallographic files in CIF format for the structure determination of complex **2**. This material is available free of charge via the Internet at <http://pubs.acs.org>.

IC051367D